# Chapter 15

# Propagation Through Random Phase Screens



**Overview:** The notion of a thin turbulent layer along a propagation path has been used for many years to model radio wave propagation through the ionosphere, scattering from a rough sea surface, or propagation of an optical wave between a satellite and the Earth's surface, among other settings. Such a turbulent layer is widely known as a *phase screen*, although this term generally refers to only a "very thin" turbulent layer. In this chapter we develop a general model for a layer of optical turbulence between a transmitter and receiver along a horizontal propagation path. If the layer is "fairly thick," it is treated much like an extended medium. However, when the ratio of the turbulent layer thickness to the propagation distance from the turbulent layer to a receiver is sufficiently small, we classify the turbulent layer as a *thin phase screen.* Basically, this means that only the phase of the optical wave is disrupted as it passes through the turbulent layer—not it's amplitude. Consequently, it is not necessary to integrate over the thickness of the layer, thus simplifying some of the expressions for various statistical quantities concerning a laser beam propagating over a path in which only a thin phase screen exists.

In our analysis we neglect the presence of extended optical turbulence and concentrate on the effects generated by the phase screen itself, taking into account the placement of the screen with respect to the transmitter and receiver. It is a straightforward extension of our model to embed the phase screen directly in an extended turbulence medium, although we don't do so here. Statistical quantities, like the mutual coherence function and scintillation index developed in Chaps. 6 and 8 for optical turbulence everywhere along the propagation path, are calculated here for the case of a single phase screen. In particular, we show how proper placement of the phase screen between the input and output planes can lead to essentially the same numerical results as that obtained from an extended turbulence model. In addition, we briefly treat the case of multiple thin phase screens that can be arbitrarily located along the propagation path. All results in this chapter, however, are limited to weak irradiance fluctuations for which the Rytov approximation is valid.

## 15.1 Introduction

For mathematical simplification, the notion of a thin random phase screen has been used as a model for studying scintillation phenomena over the years. For example, satellite radio communications through the ionosphere and the reflection of electromagnetic waves from a rough sea surface have been modeled by using phase screens [1]. In some cases, a random medium that extends between transmitter and receiver can be approximated by a thin phase screen located between the optical source and receiver. Booker et al. [2] showed that this latter approximation is valid for a plane wave incident on a random phase screen provided the screen is centrally located with respect to the extended medium and has the same refractive-index spectrum and phase variance as the extended medium. By numerically solving the fourth-moment equation, Booker et al. [2] made a comprehensive comparison of scintillation theories between the extended random medium and the phase screen model. The results from several early studies regarding a random phase screen approximation are summarized in the review by Yakushkin [3].

The phase screen analysis presented in Ref. [2] was extended to a Gaussian-beam wave by Andrews et al. [4]. In this latter study, the general model for the phase screen consisted of a slab of random medium arbitrarily located between source and receiver, as illustrated in Fig. 15.1.

Following Ref. [4], it is assumed the transmitter is located at $z = 0$ and propagation is along the positive $z$-axis. It is further assumed that the random medium exists only between the planes $z = L_1$ and $z = L_1 + L_2$ and that the receiver is located at $z = L$, where $L = L_1 + L_2 + L_3$. The phase screen is classified as "thin" under the condition $L_2/L_3 \ll 1$, which permits significant simplifications in the calculations. For the thin phase screen model, various statistical quantities associated with a transmitted Gaussian-beam wave are presented here and compared with results from Chaps. 6 and 8 for propagation through a random

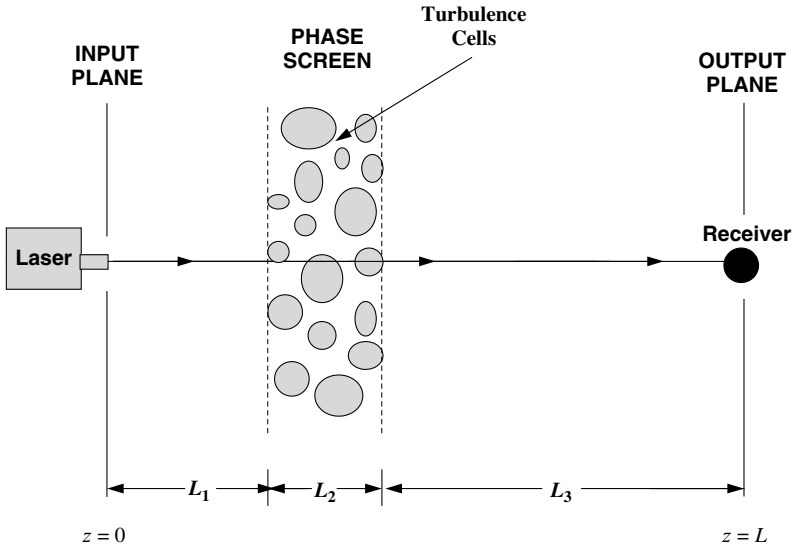


**Figure 15.1** Propagation geometry for a random phase screen.

medium fully extended between source and receiver. All calculations are based on weak fluctuation theory using the Rytov approximation.

## 15.2 Random Phase Screen Models

As in Chaps. 6 and 8, we assume the basic optical wave at the transmitter in the plane $z = 0$ is a lowest-order $\mathrm{TEM}_{00}$ *Gaussian-beam wave* with unit amplitude on the optical axis. Such a wave is characterized by

$$U_0(\mathbf{r}, 0) = \exp\left(-\frac{r^2}{W_0^2} - i\frac{kr^2}{2F_0}\right), \tag{1}$$

where $W_0$ and $F_0$ denote the *spot size radius* and *phase front radius of curvature*, respectively; $r$ is distance in the transverse direction; and $k = 2\pi/\lambda$ is the optical wave number. If a random medium exists along any part of the propagation path between transmitter and receiver, the optical field at distance $z = L$ from the transmitter under the *Rytov approximation* is (see Chap. 5)

$$U(\mathbf{r}, L) = U_0(\mathbf{r}, L)\exp\left[\psi_1(\mathbf{r}, L) + \psi_2(\mathbf{r}, L) + \cdots\right], \tag{2}$$

where

$$U_0(\mathbf{r}, L) = \frac{1}{\Theta_0 + i\,\Lambda_0}\exp\left(ikL - \frac{r^2}{W^2} - i\frac{kr^2}{2F}\right) \tag{3}$$

is the optical wave in the absence of turbulence and $\psi_1(\mathbf{r}, L)$ and $\psi_2(\mathbf{r}, L)$ are first-order and second-order *complex phase perturbations* caused by the random

medium. The multiplicative factor $1/(\Theta_0 + i\,\Lambda_0)$ in front of the right-hand side of (3) is the complex amplitude, which identifies the input-plane beam parameters

$$\Theta_0 = 1 - \frac{L}{F_0}, \quad \Lambda_0 = \frac{2L}{kW_0^2}. \tag{4}$$

The quantities $W$ and $F$ are the *beam spot-size radius* and *phase front radius of curvature* at the receiver defined by the output-plane beam parameters (Section 4.3)

$$\begin{aligned} \Theta &= 1 + \frac{L}{F} = \frac{\Theta_0}{\Theta_0^2 + \Lambda_0^2}, \quad \bar{\Theta} = 1 - \Theta, \\ \Lambda &= \frac{2L}{kW^2} = \frac{\Lambda_0}{\Theta_0^2 + \Lambda_0^2}. \end{aligned} \tag{5}$$

We begin by recalling the second-order moments [Eqs. (15)–(17) in Chap. 6]

$$E_1(0,0) = -2\pi^2 k^2 \int_0^L \int_0^\infty \kappa \Phi_n(\kappa, z) d\kappa\, dz, \tag{6}$$

$$\begin{aligned} E_2(\mathbf{r}_1, \mathbf{r}_2) = 4\pi^2 k^2 &\int_0^L \int_0^\infty \kappa \Phi_n(\kappa, z) \exp\left[-\frac{\Lambda L \kappa^2 (1 - z/L)^2}{k}\right] \\ &\times J_0\left\{\kappa\left|\left[1 - \overline{\Theta}(1 - z/L)\right]\mathbf{p} - 2i\Lambda(1 - z/L)\mathbf{r}\right|\right\} d\kappa\, dz, \end{aligned} \tag{7}$$

$$\begin{aligned} E_3(\mathbf{r}_1, \mathbf{r}_2) = -4\pi^2 k^2 &\int_0^L \int_0^\infty \kappa \Phi_n(\kappa, z) \exp\left[-\frac{\Lambda L \kappa^2 (1 - z/L)^2}{k}\right] \\ &\times \exp\left\{-\frac{iL\kappa^2}{k}(1 - z/L)\left[1 - \overline{\Theta}(1 - z/L)\right]\right\} \\ &\times J_0\left\{\kappa\rho\left[1 - (\overline{\Theta} + i\Lambda)(1 - z/L)\right]\right\} d\kappa\, dz. \end{aligned} \tag{8}$$

As before, $\Phi_n(\kappa, z)$ is the spatial power spectrum of refractive-index fluctuations that is nonzero along some portion of the propagation path, $\mathbf{r} = \frac{1}{2}(\mathbf{r}_1 + \mathbf{r}_2)$, $\mathbf{p} = \mathbf{r}_1 - \mathbf{r}_2$, $\rho = |\mathbf{p}|$, and $J_0(x)$ is a Bessel function (see Appendix I). Below, we consider separately the turbulent layer model of arbitrary thickness and that defined as a thin phase screen.

### 15.2.1 Turbulent layer of arbitrary thickness

Because the random medium in Fig. 15.1 is assumed to exist along the propagation path only over the interval $L_1 \le z \le L_1 + L_2$, we set $\Phi_n(\kappa, z) = 0, 0 \le z < L_1$, $L_1 + L_2 < z \le L$. Thus, it is convenient to introduce the normalized distance variable $\eta$ by

$$1 - \frac{z}{L} = d_3(1 + d_2\eta), \qquad 0 \le \eta \le 1, \tag{9}$$

where $d_2 = L_2/L_3$ and $d_3 = L_3/L$. This notation changes Eqs. (6)–(8) to

$$E_1(0,0) = -2\pi^2 k^2 L d_2 d_3 \int_0^1 \int_0^\infty \kappa \Phi_n(\kappa,\eta) d\kappa\, d\eta, \tag{10}$$

$$E_2(\mathbf{r}_1,\mathbf{r}_2) = 4\pi^2 k^2 L d_2 d_3 \int_0^1 \int_0^\infty \kappa \Phi_n(\kappa,\eta) \exp\left[-\frac{\Lambda L \kappa^2 d_3^2 (1+d_2\eta)^2}{k}\right] \times J_0\left\{\kappa\left|\left[1-\overline{\Theta} d_3(1+d_2\eta)\right]\mathbf{p} - 2i\Lambda d_3(1+d_2\eta)\mathbf{r}\right|\right\} d\kappa\, d\eta, \tag{11}$$

$$E_3(\mathbf{r}_1,\mathbf{r}_2) = -4\pi^2 k^2 L d_2 d_3 \int_0^1 \int_0^\infty \kappa \Phi_n(\kappa,\eta) \exp\left[-\frac{\Lambda L \kappa^2 d_3^2 (1+d_2\eta)^2}{k}\right] \times \exp\left\{-\frac{iL\kappa^2}{k} d_3(1+d_2\eta)\left[1-\overline{\Theta} d_3(1+d_2\eta)\right]\right\} \times J_0\left\{\kappa\rho\left[1-(\overline{\Theta}+i\Lambda) d_3(1+d_2\eta)\right]\right\} d\kappa\, d\eta. \tag{12}$$

It is interesting to consider the above expressions for the limiting cases $d_3 = 0$ and $d_3 = 1$. The first case $d_3 = 0$ corresponds to the placement of the turbulent layer directly in front of the receiver. If the turbulent layer is far from the optical source ($L_2/L_1 \ll 1$), then Eqs. (10)–(12) in the limit $d_3 = 0$ reduce to the *plane wave* expressions

$$E_1(0,0) = -2\pi^2 k^2 L_2 \int_0^1 \int_0^\infty \kappa \Phi_n(\kappa,\eta) d\kappa\, d\eta, \tag{13}$$

$$E_2(\mathbf{r}_1,\mathbf{r}_2) = 4\pi^2 k^2 L_2 \int_0^1 \int_0^\infty \kappa \Phi_n(\kappa,\eta) J_0(\kappa\rho) d\kappa\, d\eta, \tag{14}$$

$$E_3(\mathbf{r}_1,\mathbf{r}_2) = -4\pi^2 k^2 L_2 \int_0^1 \int_0^\infty \kappa \Phi_n(\kappa,\eta) \exp\left(-\frac{iL_2\kappa^2\eta}{k}\right) \times J_0(\kappa\rho) d\kappa\, d\eta. \tag{15}$$

Hence, regardless of the initial form of the optical wave, the wave incident on the turbulent layer behaves much like a plane wave. Among other applications, the limiting case $d_3 = 0$ occurs in astronomy where the source (star) is far from the random medium (Earth's atmosphere) in which the ground receiver is located. The other limiting case $d_3 = 1$ corresponds to the turbulent layer placed at the source. This latter case arises, for example, in an uplink communications system in which the transmitter is located near ground level whereas the receiver is far above the Earth's atmosphere. The optical wave in this case cannot be approximated by a simple plane wave model.

### 15.2.2 Thin phase screen

A turbulent slab is characterized as a "thin" phase screen if its thickness is much smaller than the propagation distance following the layer, i.e., if $d_2 \ll 1$. This is the case most used in practice. Although we do not explicitly make the assumption, most thin phase screen models assume that only the phase is disrupted by the random slab, not the amplitude.

Under the assumption of a thin phase screen, we can set $1 + d_2 \cong 1$, which eliminates the dependency on propagation distance $z$. Consequently, $\Phi_n(\kappa, z) = \Phi_n(\kappa)$ and Eqs. (10)–(12) reduce to the single integral expressions

$$E_1(0,0) = -2\pi^2 k^2 L d_2 d_3 \int_0^\infty \kappa \Phi_n(\kappa)\, d\kappa, \tag{16}$$

$$\begin{aligned} E_2(\mathbf{r}_1, \mathbf{r}_2) = {} & 4\pi^2 k^2 L d_2 d_3 \int_0^\infty \kappa \Phi_n(\kappa) \exp\left(-\frac{\Lambda L \kappa^2 d_3^2}{k}\right) \\ & \times J_0\left[\kappa |(1 - \overline{\Theta} d_3)\mathbf{p} - 2i\Lambda d_3 \mathbf{r}|\right] d\kappa, \end{aligned} \tag{17}$$

$$\begin{aligned} E_3(\mathbf{r}_1, \mathbf{r}_2) = {} & -4\pi^2 k^2 L d_2 d_3 \int_0^\infty \kappa \Phi_n(\kappa) \exp\left(-\frac{\Lambda L \kappa^2 d_3^2}{k}\right) \\ & \times \exp\left[-\frac{iL\kappa^2}{k} d_3(1 - \overline{\Theta} d_3)\right] J_0\left[\kappa\rho(1 - \overline{\Theta} d_3 - i\Lambda d_3)\right] d\kappa. \end{aligned} \tag{18}$$

### 15.2.3 Relation to an extended medium

To equate a thin random phase screen model with an extended random medium model in the case of a plane wave, the phase screen should be placed midway between source and receiver (i.e., set $d_3 = L_3/L = 0.5$). In addition, the Rytov variance for the phase screen model should be equated with that for the extended random medium model.

For an extended random medium over a propagation path of length $L$, the Rytov variance is defined by (Section 8.2)

$$\begin{aligned} \sigma_R^2 &= 8\pi^2 k^2 L \int_0^1 \int_0^\infty \kappa \Phi_n(\kappa) \left[1 - \cos\left(\frac{L\kappa^2 \xi}{k}\right)\right] d\kappa\, d\xi \\ &= 1.23 C_n^2 k^{7/6} L^{11/6}, \end{aligned} \tag{19}$$

where the spatial power spectrum of refractive-index fluctuations is the Kolmogorov spectrum. For a thin random phase screen and Kolmogorov spectrum, where $\hat{c}_n^2$ is the refractive-index structure constant of the phase screen, the comparable expression is [4–6]

$$\begin{aligned}\hat{\sigma}_R^2 &= 8\pi^2 k^2 L d_2 d_3 \int_0^\infty \kappa \Phi_n(\kappa)\left[1 - \cos\left(\frac{L\kappa^2 d_3}{k}\right)\right] d\kappa \\ &= 2.25\hat{c}_n^2 k^{7/6} L^{11/6} d_2 d_3^{11/6}.\end{aligned} \tag{20}$$

By enforcing the equivalence of Eqs. (19) and (20), we are led to the relation between structure constants given by

$$C_n^2 = 1.83 d_2 d_3^{11/6} \hat{c}_n^2 = 1.83 d_3^{5/6} \frac{L_2}{L} \hat{c}_n^2. \tag{21}$$

Equation (21) identifies an equivalence between the extended turbulence structure constant $C_n^2$ and the phase screen structure constant $\hat{c}_n^2$, the latter dependent on the thickness $L_2$ of the screen and the distance the wave propagates behind the screen. Thus, if the thin phase screen is moved next to the receiver ($d_3 \sim 0$), the equivalent structure constant $C_n^2$ approaches zero. In this latter case, no intensity fluctuations are associated with the optical wave as it emerges from the screen; such fluctuations arise only after the wave has propagated a certain distance behind the screen. This result is in sharp contrast with the thick turbulent slab observations previously discussed.

## 15.3 Mutual Coherence Function

Assuming a thin random phase screen model and Kolmogorov spectrum, the MCF [Eq. (33) in Chap. 6] can be evaluated in this case to give

$$\begin{aligned}\Gamma_2(\mathbf{r}_1, \mathbf{r}_2, L) &= \Gamma_2^0(\mathbf{r}_1, \mathbf{r}_2, L) \exp[2E_1(0,0) + E_2(\mathbf{r}_1, \mathbf{r}_2)] \\ &= \Gamma_2^0(\mathbf{p}, \mathbf{r}, L) \exp\left\{ -1.93\hat{\sigma}_R^2 (\Lambda d_3)^{5/6} \right. \\ &\quad \left. \times {}_1F_1\left[-\frac{5}{6}; 1; -\frac{k|(1 - \overline{\Theta} d_3)\mathbf{p} - 2i\Lambda d_3 \mathbf{r}|^2}{4\Lambda L d_3^2}\right]\right\},\end{aligned} \tag{22}$$

where ${}_1F_1(a;c;x)$ is the confluent hypergeometric function (see Appendix I). Equation (22) is an exact result for the phase screen model. However, for many situations we can use the large argument asymptotic formula of the confluent hypergeometric function to obtain the simpler formulation

$$\Gamma_2(\mathbf{p}, \mathbf{r}, L) = \Gamma_2^0(\mathbf{p}, \mathbf{r}, L) \exp\left[-0.65\hat{\sigma}_R^2 \left(\frac{k}{L d_3}\right)^{5/6} \left|(1 - \overline{\Theta} d_3)\mathbf{p} - 2i\Lambda d_3 \mathbf{r}\right|^{5/3}\right], \quad \rho > \sqrt{L/k}. \tag{23}$$

Moreover, in the special case $\mathbf{r}_2 = -\mathbf{r}_1$, the MCF (23) normalized by its on-axis value simplifies to

$$\frac{\Gamma_2(\rho, L)}{\Gamma_2(0, L)} = \exp\left[-\frac{\Lambda}{4}\left(\frac{k\rho^2}{L}\right) - 0.65\hat{\sigma}_R^2\left|1 - \overline{\Theta}d_3\right|^{5/3}\left(\frac{k\rho^2}{Ld_3}\right)^{5/6}\right], \quad \rho > \sqrt{L/k}. \tag{24}$$

Equation (24) is plotted in Fig. 15.2 (dotted curves) as a function of $(k\rho^2/L)^{1/2}$ for three collimated beams and compared with results (solid curves) derived from the extended turbulence model in Chap. 6.

The strength of turbulence for the extended-turbulence model and the phase screen model are characterized by $\sigma_R^2 = \hat{\sigma}_R^2 = 0.2$. The close comparison between the phase screen result and that associated with extended turbulence is achieved by properly selecting the position of the phase screen. In this case we have used the empirical formula

$$d_3 = 0.46 + 0.04\Theta. \tag{25}$$

Equation (25) leads to $d_3 = 0.46$ for a spherical wave ($\Theta = \Lambda = 0$) and to $d_3 = 0.5$ for an unbounded plane wave ($\Theta = 1, \Lambda = 0$). Hence, to equate the phase screen expression (24) with that of extended turbulence, the position of the phase screen must vary such that $0.46 < d_3 < 0.5$ in the general case of a collimated Gaussian-beam wave. Except for small beams, the distinction between this upper and lower bound on $d_3$ is not very significant.

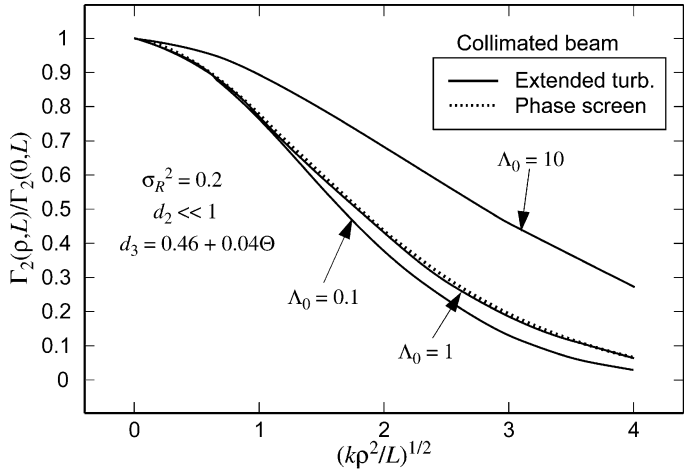


**Figure 15.2** The normalized MCF plotted as a function of $\rho$ scaled by the first Fresnel zone for three collimated beams. The solid curves correspond to numerical results based on an extended-turbulence model [Eq. (54) in Chap. 6] and the dotted curves represent Eq. (24) for the case of a thin random phase screen.

### 15.3.1 Mean irradiance

For $\mathbf{r}_1 = \mathbf{r}_2 = \mathbf{r}$, the *mean irradiance* deduced from (22) can be written as (Section 6.3)

$$\begin{aligned}\langle I(\mathbf{r}, L)\rangle &= \Gamma_2(\mathbf{r}, \mathbf{r}, L)\\ &= \frac{W_0^2}{W^2}\exp\left(-\frac{2r^2}{W^2}\right)\exp\left[2\sigma_r^2(\mathbf{r}, L) - T\right],\end{aligned} \tag{26}$$

where

$$T = 1.93\,\hat{\sigma}_R^2(\Lambda d_3)^{5/6}, \tag{27}$$

$$\begin{aligned}\sigma_r^2(\mathbf{r}, L) &= 0.97\,\hat{\sigma}_R^2(\Lambda d_3)^{5/6}\left[1 - {}_1F_1\left(-\frac{5}{6}; 1; \frac{2r^2}{W^2}\right)\right]\\ &\cong 1.61\,\hat{\sigma}_R^2(\Lambda d_3)^{5/6}\frac{r^2}{W^2}, \quad r < W.\end{aligned} \tag{28}$$

As before, we assume the mean irradiance is approximated by the Gaussian profile

$$\langle I(\mathbf{r}, L)\rangle \cong \frac{W_0^2}{W_{\mathrm{LT}}^2}\exp\left(-\frac{2r^2}{W_{\mathrm{LT}}^2}\right), \tag{29}$$

where the effective or long-term spot size for a thin phase screen and that for extended turbulence are given by

$$\begin{aligned}W_{\mathrm{LT}} &= W\sqrt{1 + T}\\ &= \begin{cases} W\sqrt{1 + 1.93\hat{\sigma}_R^2(\Lambda d_3)^{5/6}}, & \text{(phase screen)},\\ W\sqrt{1 + 1.33\sigma_R^2\Lambda^{5/6}}, & \text{(extended turbulence)}.\end{cases}\end{aligned} \tag{30}$$

Here, equality of the two expressions in (30) is achieved only by placing the phase screen such that $d_3 = 0.64$.

### 15.3.2 Spatial coherence radius

The spatial coherence radius is deduced from knowledge of the *modulus of the complex degree of coherence* (DOC) defined by

$$\begin{aligned}\mathrm{DOC}(\mathbf{r}_1, \mathbf{r}_2, L) &= \frac{|\Gamma_2(\mathbf{r}_1, \mathbf{r}_2, L)|}{\sqrt{\langle I(\mathbf{r}_1, L)\rangle}\sqrt{\langle I(\mathbf{r}_2, L)\rangle}}\\ &= \exp\left[-\frac{1}{2}D(\mathbf{r}_1, \mathbf{r}_2, L)\right],\end{aligned} \tag{31}$$

where $D(\mathbf{r}_1, \mathbf{r}_2, L) \equiv D(\mathbf{p}, \mathbf{r}, L)$ is the wave structure function (WSF). Based on the above expressions, the WSF can be written as

$$D(\mathbf{p},\mathbf{r},L) = 3.87\hat{\sigma}_R^2(\Lambda d_3)^{5/6}\mathrm{Re}\left\{{}_1F_1\left[-\frac{5}{6};1;\ -\frac{k|(1-\overline{\Theta}d_3)\mathbf{p}-2i\Lambda d_3\mathbf{r}|^2}{4\Lambda L d_3^2}\right]\right.$$
$$\left.-\frac{1}{2}{}_1F_1\left(-\frac{5}{6};1;\ \frac{2|\mathbf{r}+\mathbf{p}/2|^2}{W^2}\right)-\frac{1}{2}{}_1F_1\left(-\frac{5}{6};1;\ \frac{2|\mathbf{r}-\mathbf{p}/2|^2}{W^2}\right)\right\}, \tag{32}$$

which, for the special case $\mathbf{r}_2 = -\mathbf{r}_1$, reduces to

$$D(\rho,L) = 3.87\hat{\sigma}_R^2(\Lambda d_3)^{5/6}\left\{{}_1F_1\left[-\frac{5}{6};1;\ -\frac{k(1-\overline{\Theta}d_3)^2\rho^2}{4\Lambda L d_3^2}\right]\right.$$
$$\left.-{}_1F_1\left(-\frac{5}{6};1;\ \frac{k\Lambda\rho^2}{4L}\right)\right\}. \tag{33}$$

For many cases of interest, the asymptotic forms for the confluent hypergeometric functions in Eq. (33) can be used to obtain the simple approximation (see Prob. 3)

$$D(\rho,L) \cong 1.30\,\hat{\sigma}_R^2 d_3^{5/6}\left[\left|\frac{1}{d_3}-\overline{\Theta}\right|^{5/3}\left(\frac{k\rho^2}{L}\right)^{5/6}+0.62\Lambda^{11/6}\left(\frac{k\rho^2}{L}\right)\right],$$
$$\rho > \sqrt{L/k}, \tag{34}$$

similar in form to Eq. (77) in Chap. 6 for the case of extended turbulence with zero inner scale.

The *spatial coherence radius* $\rho_0$ is defined by the $e^{-1}$ point of the DOC (31). Hence, the implied spatial coherence radius deduced from Eq. (34) can be expressed as

$$\frac{\rho_0}{\rho_{\mathrm{pl}}} \cong \left(\left|1-\overline{\Theta}d_3\right|^{5/3}+0.62d_3^{5/3}\Lambda^{11/6}\right)^{-3/5}, \quad \rho_0 > \sqrt{L/k}, \tag{35}$$

where $\rho_{\mathrm{pl}}$ is the plane wave coherence radius ($\Theta = 1$, $\Lambda = 0$). In arriving at Eq. (35), we have used the approximation $k\rho^2/L \cong (k\rho^2/L)^{5/6}$.

Spatial coherence radii implied by relations (35) above and (78) in Chap. 6 for a collimated Gaussian-beam wave are shown in Fig. 15.3 as a function of the Fresnel ratio $\Lambda_0$ at the transmitter. The similarity of numerical results from the two models is obtained by choosing $d_3$ once again according to the empirical formula (25).

## 15.4 Scintillation Index and Covariance Function

Fluctuations in the irradiance are described by the *normalized variance* of the irradiance, or *scintillation inde*x, which, for the thin phase screen (model) under weak irradiance fluctuations, leads to

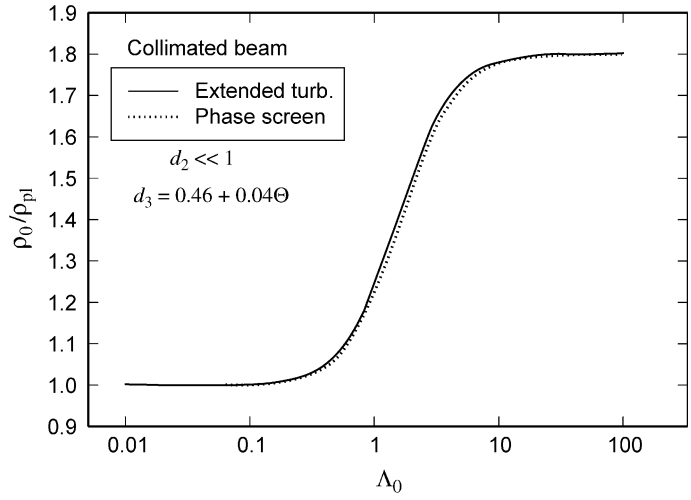


**Figure 15.3** The spatial coherence radius $\rho_0$ of a collimated beam passing through a thin random phase screen, scaled by the plane wave coherence radius $\rho_{pl}$ and plotted as a function of $\Lambda_0 = 2L/kW_0^2$. The extended medium case from Chap. 6 is also shown (solid curve).

$$\begin{aligned}\sigma_I^2(\mathbf{r}, L) &= 2\ \mathrm{Re}[E_2(\mathbf{r}, \mathbf{r}) + E_3(\mathbf{r}, \mathbf{r})] \\ &= 8\pi^2 k^2 L d_2 d_3 \int_0^\infty \kappa \Phi_n(\kappa) \exp\left(-\frac{\Lambda L \kappa^2 d_3^2}{k}\right) \\ &\quad \times \left\{ I_0(2\Lambda d_3 \kappa r) - \cos\left[\frac{L\kappa^2 d_3}{k}\left(1 - \overline{\Theta} d_3\right)\right]\right\} d\kappa. \end{aligned} \tag{36}$$

Under the assumption of a Kolmogorov spectrum, Eq. (36) can be approximated by

$$\begin{aligned}\sigma_I^2(\mathbf{r}, L) = 6.45\, \hat{\sigma}_R^2 (\Lambda d_3)^{5/6} \left(\frac{r^2}{W^2}\right) + 3.87\, \hat{\sigma}_R^2 \left\{ \left[ (\Lambda d_3)^2 + \left(1 - \overline{\Theta} d_3\right)^2 \right]^{5/12} \right. \\ \left. \times \cos\left[\frac{5}{6} \tan^{-1}\left(\frac{1 - \overline{\Theta} d_3}{\Lambda d_3}\right)\right] - (\Lambda d_3)^{5/6} \right\}, \quad r < W. \end{aligned} \tag{37}$$

To establish an equivalence between Eq. (37) and Eq. (23) in Chap. 8 for the case of an extended medium, the phase screen must be located according to the empirical relation

$$d_3 = 0.67 - 0.17\Theta. \tag{38}$$

Note that (38) is not the same relation cited for the MCF [recall Eq. (25)]. In particular, whereas Eq. (38) leads to $d_3 = 0.5$ for a plane wave, it defines $d_3 = 0.67$ for a spherical wave. In the case of a collimated beam, this requires $0.5 < d_3 < 0.67$. We may conclude, therefore, that to equate scintillation theories between a phase screen and extended turbulence, the screen must be closer to the transmitter for a Gaussian-beam wave than for a plane wave. In Fig. 15.4 the

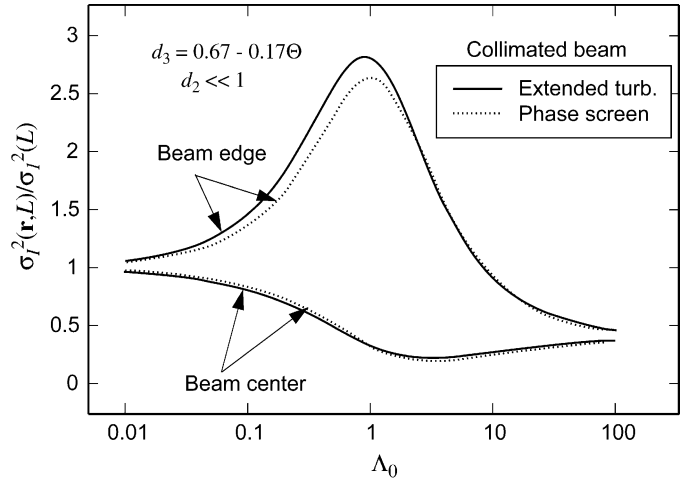


**Figure 15.4** The dashed curves denote the scaled scintillation index for a collimated beam passing through a thin random phase screen and plotted as a function of $\Lambda_0 = 2L/kW_0^2$. The solid curves represent the scintillation index for an extended-turbulence model.

scintillation index predicted by Eq. (37) above and Eq. (23) in Chap. 8 is shown at the optical axis of the beam and also at the diffraction-limited beam edge ($r = W$). Once again, the two models predict similar results everywhere with the greatest deviation being off-axis where $\Lambda_0 < 1$.

The *covariance function* of the irradiance identifies the spatial correlation width $\rho_c$ for the irradiance fluctuations. In the case of a thin random phase screen, it is defined by

$$B_I(\mathbf{p},\mathbf{r},L) = 8\pi^2 k^2 L d_2 d_3 \int_0^\infty \kappa\Phi_n(\kappa)\exp\left(-\frac{\Lambda L d_3^2\kappa^2}{k}\right)$$
$$\times \mathrm{Re}\left\{J_0\big[\kappa\big|(1-\overline{\Theta}d_3)\mathbf{p} - 2i\Lambda d_3\mathbf{r}\big|\big]\right.$$
$$\left. - \exp\left[-\frac{iL\kappa^2 d_3}{k}\left(1-\overline{\Theta}d_3\right)\right]J_0\big[\kappa\rho(1-\overline{\Theta}d_3 - i\Lambda d_3)\big]\right\} d\kappa. \quad (39)$$

Based on the Kolmogorov spectrum, the evaluation of the integral in Eq. (39) yields the exact expression

$$B_I(\mathbf{p},\mathbf{r},L) = 3.87\hat{\sigma}_R^2 \mathrm{Re}\left\{ i^{5/6}\big[1-(\overline{\Theta}+i\Lambda)d_3\big]_1^{5/6} F_1\left[-\frac{5}{6};1;\frac{\left(1-\overline{\Theta}d_3 - i\Lambda d_3\right)k\rho^2}{4iLd_3}\right]\right.$$
$$\left. -(\Lambda d_3)^{5/6}{}_1F_1\left[-\frac{5}{6};1;-\frac{k|(1-\overline{\Theta}d_3)\mathbf{p} - 2i\Lambda d_3\mathbf{r}|^2}{4L\Lambda d_3^2}\right]\right\} \quad (40)$$

Here we see that the covariance function is statistically inhomogeneous, i.e., it depends on the location of the two points—not simply their separation distance.

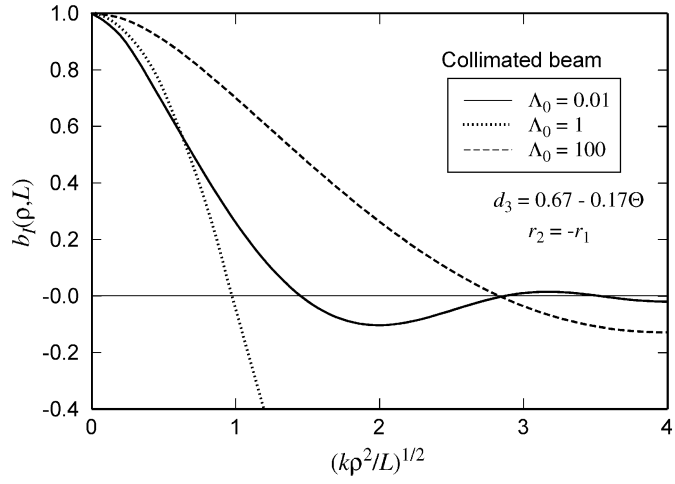


**Figure 15.5** The normalized covariance function for three colimated beams plotted as a function of the normalized distance $(k\rho^2/L)^{1/2}$.

However, the argument in the second confluent hypergeometric function in Eq. (40) can be simplified in the special case for which the observation points satisfy $\mathbf{r}_2 = -\mathbf{r}_1$, resulting in the expression

$$B_I(\rho, L) = 3.87\hat{\sigma}_R^2 \,\mathrm{Re}\left\{ i^{5/6}\left[1 - (\overline{\Theta} + i\Lambda)d_3\right]^{5/6} {}_1F_1\left[-\frac{5}{6}; 1; -\frac{(1 - \overline{\Theta}d_3 - i\Lambda d_3)k\rho^2}{4iLd_3}\right] \right.$$
$$\left. - (\Lambda d_3)^{5/6} {}_1F_1\left[-\frac{5}{6}; 1; -\frac{(1 - \overline{\Theta}d_3)k\rho^2}{4L\Lambda d_3^2}\right]\right\}. \tag{41}$$

In the limiting cases of a plane wave and spherical wave, Eq. (41) reduces to Eqs. (51) and (52), respectively, in Chap. 8. Also, for further computational ease, both confluent hypergeometric functions in (41) can be closely approximated by the simple algebraic expression (61) in Chap. 6, which is valid for certain complex arguments $x$ as well as real arguments. In Fig. 15.5 we plot the normalized covariance function $b_I(\rho, L) = B_I(\rho, L)/B_I(0, L)$ as a function of $(k\rho^2/L)^{1/2}$ for three types of collimated beam. The case $\Lambda_0 = 0.01$ is similar to that of a plane wave whereas the case $\Lambda_0 = 100$ is similar to that of a spherical wave. In all cases the phase screen is positioned according to Eq. (38), the same as that for the scintillation index. By choosing $d_3$ in this manner, the results are comparable with those for an extended random medium between source and receiver (see Fig. 8.9).

## 15.5 Multiple Phase Screens

The case of multiple random phase screens can be treated in a manner analogous to that of a single phase screen. However, to satisfy the limitations of weak fluctuation theory, we must assume that the strength of each phase screen decreases

appropriately as the number of phase screens is increased. The following discussion is based on such an assumption.

To begin, consider two random phase screens as illustrated in Fig. 15.6. Following the approach used in Section 15.2 now leads to the second-order moments

$$E_1(0,0) = -2\pi^2 k^2 L d_2 d_3 \int_0^1 \int_0^\infty \kappa \Phi_n(\kappa,\eta) d\kappa\, d\eta - 2\pi^2 k^2 L d_4 d_5 \int_0^1 \int_0^\infty \kappa \Phi_n(\kappa,\eta) d\kappa\, d\eta, \tag{42}$$

$$\begin{aligned} E_2(\mathbf{r}_1,\mathbf{r}_2) = {} & 4\pi^2 k^2 L d_2 d_3 \int_0^1 \int_0^\infty \kappa \Phi_n(\kappa,\eta) \exp\left[-\frac{\Lambda L \kappa^2 d_3^2 (1+d_2\eta)^2}{k}\right] \\ & \times J_0\left\{\kappa\left|\left[1-\overline{\Theta} d_3(1+d_2\eta)\right]\mathbf{p} - 2i\Lambda d_3(1+d_2\eta)\mathbf{r}\right|\right\} d\kappa\, d\eta \\ & + 4\pi^2 k^2 L d_4 d_5 \int_0^1 \int_0^\infty \kappa \Phi_n(\kappa,\eta) \exp\left[-\frac{\Lambda L \kappa^2 d_5^2 (1+d_4\eta)^2}{k}\right] \\ & \times J_0\left\{\kappa\left|\left[1-\overline{\Theta} d_5(1+d_4\eta)\right]\mathbf{p} - 2i\Lambda d_5(1+d_4\eta)\mathbf{r}\right|\right\} d\kappa\, d\eta, \end{aligned} \tag{43}$$

$$\begin{aligned} E_3(\mathbf{r}_1,\mathbf{r}_2) = {} & -4\pi^2 k^2 L d_2 d_3 \int_0^1 \int_0^\infty \kappa \Phi_n(\kappa,\eta) \exp\left[-\frac{\Lambda L \kappa^2 d_3^2 (1+d_2\eta)^2}{k}\right] \\ & \times \exp\left\{-\frac{iL\kappa^2}{k} d_3(1+d_2\eta)\left[1-\overline{\Theta} d_3(1+d_2\eta)\right]\right\} \\ & \times J_0\left\{\kappa\rho\left[1-(\overline{\Theta}+i\Lambda) d_3(1+d_2\eta)\right]\right\} d\kappa\, d\eta \\ & - 4\pi^2 k^2 L d_4 d_5 \int_0^1 \int_0^\infty \kappa \Phi_n(\kappa,\eta) \exp\left[-\frac{\Lambda L \kappa^2 d_5^2 (1+d_4\eta)^2}{k}\right] \\ & \times \exp\left\{-\frac{iL\kappa^2}{k} d_5(1+d_4\eta)\left[1-\overline{\Theta} d_5(1+d_4\eta)\right]\right\} \\ & \times J_0\left\{\kappa\rho\left[1-(\overline{\Theta}+i\Lambda) d_5(1+d_4\eta)\right]\right\} d\kappa\, d\eta, \end{aligned} \tag{44}$$

where $L = L_1 + L_2 + L_3 + L_4 + L_5$, the thickness of each phase screen is totally arbitrary, and

$$d_2 = \frac{L_2}{L_3}, \quad d_3 = \frac{L_3}{L}, \quad d_4 = \frac{L_4}{L_5}, \quad d_5 = \frac{L_5}{L}. \tag{45}$$

For the case in which both random phase screens are thin, we can simply set $1 + d_2 \cong 1$ and $1 + d_4 \cong 1$ as before. This condition implies that the distance behind each phase screen is much greater than the thickness of the screen.

Equations (42)–(44) are easily generalized to the case of $N$ random phase screens. For example, consider the special case in which $N$ identical thin random

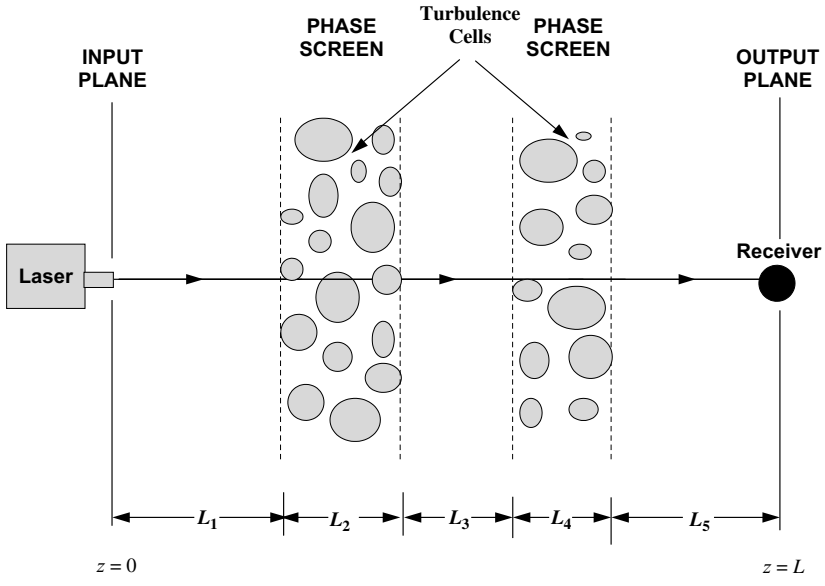


**Figure 15.6** Propagation geometry for two random phase screens.

phase screens are equally spaced between source and receiver. In this case, we write $\hat{d}_1 \equiv d_1 = d_3 = \cdots = d_{2N+1} = 1/(N+1)$, $d_2 = d_4 = \cdots = d_{2N} \equiv \hat{d}_2/N$,

$$E_1(0,0) = -2\pi^2 k^2 L(\hat{d}_1\hat{d}_2)\int_0^\infty \kappa\Phi_n(\kappa)d\kappa, \tag{46}$$

$$E_2(\mathbf{r}_1,\mathbf{r}_2) = 4\pi^2 k^2 L(\hat{d}_1\hat{d}_2)\int_0^\infty \kappa\Phi_n(\kappa)\exp\left(-\frac{\Lambda L\kappa^2\hat{d}_1^2}{k}\right) \times J_0\Big[\kappa|(1-\overline{\Theta}\hat{d}_1)\mathbf{p} - 2i\Lambda\hat{d}_1\mathbf{r}|\Big]d\kappa, \tag{47}$$

$$E_3(\mathbf{r}_1,\mathbf{r}_2) = -4\pi^2 k^2 L(\hat{d}_1\hat{d}_2)\int_0^\infty \kappa\Phi_n(\kappa)\exp\left(-\frac{\Lambda L\kappa^2\hat{d}_1^2}{k}\right) \times \exp\left[-\frac{iL\kappa^2}{k}\hat{d}_1(1-\overline{\Theta}\hat{d}_1)\right]J_0\Big[\kappa\rho(1-\overline{\Theta}\hat{d}_1 - i\Lambda\hat{d}_1)\Big]d\kappa, \tag{48}$$

where $\hat{d}_2 < 1$ and $N = 1, 2, 3, \ldots$. In the limit $N \to \infty$, Eqs. (46)–(48) reduce to those of a plane wave provided the distance from the source to the first phase screen remains much greater than the thickness of the phase screen. Hence, for sufficiently large $N$, all statistical quantities reduce to those associated with an unbounded plane wave propagating through extended turbulence.

## 15.6 Summary and Discussion

In many examples involving line-of-sight propagation on horizontal paths, the atmospheric turbulence between transmitter and receiver can be replaced by a thin random phase screen model. The thin phase screen model is particularly interesting because its simpler mathematical formulation leads to exact analytic results for the field moments that, through proper placement of the phase screen between transmitter and receiver, can be equated to field moments associated with a Gaussian-beam wave propagating through an extended random medium. This relation between phase screens and extended turbulence carries special significance because exact results for the field moments for the extended turbulence model have not thus far been produced except in some limiting cases such as unbounded plane waves and spherical waves.

The main results presented here include exact expressions for the statistical quantities of greatest interest. These include the MCF

$$\Gamma_2(\mathbf{p},\mathbf{r},L)=\Gamma_2^0(\mathbf{p},\mathbf{r},L)\exp\Bigg\{-1.93\hat{\sigma}_R^2(\Lambda d_3)^{5/6} \times {}_1F_1\bigg[-\frac{5}{6};1;-\frac{k|(1-\overline{\Theta}d_3)\mathbf{p}-2i\Lambda d_3\mathbf{r}|^2}{4\Lambda L d_3^2}\bigg]\Bigg\}, \tag{49}$$

the WSF

$$D(\mathbf{p},\mathbf{r},L)=3.87\hat{\sigma}_R^2(\Lambda d_3)^{5/6}\mathrm{Re}\Bigg\{{}_1F_1\bigg[-\frac{5}{6};1;-\frac{k|(1-\overline{\Theta}\,d_3)^2\mathbf{p}-2i\Lambda d_3\mathbf{r}|^2}{4\Lambda L d_3^2}\bigg] -\frac{1}{2}{}_1F_1\bigg(-\frac{5}{6};1;\frac{2|\mathbf{r}+\mathbf{p}/2|^2}{W^2}\bigg)-\frac{1}{2}{}_1F_1\bigg(-\frac{5}{6};1;\frac{2|\mathbf{r}-\mathbf{p}/2|^2}{W^2}\bigg)\Bigg\}, \tag{50}$$

and the covariance function of irradiance fluctuations

$$B_I(\mathbf{p},\mathbf{r},L)=3.87\hat{\sigma}_R^2\mathrm{Re}\Bigg\{\big[\Lambda d_3+i(1-\overline{\Theta}d_3)\big]^{5/6} \times {}_1F_1\bigg[-\frac{5}{6};1;-\frac{(1-\overline{\Theta}d_3-i\Lambda d_3)^2k\rho^2}{4Ld_3[\Lambda d_3+i(1-\overline{\Theta}d_3)]}\bigg] -(\Lambda d_3)^{5/6}{}_1F_1\bigg[-\frac{5}{6};1;-\frac{k|(1-\overline{\Theta}d_3)\mathbf{p}-2i\Lambda d_3\mathbf{r}|^2}{4L\Lambda d_3^2}\bigg]\Bigg\}. \tag{51}$$

The scintillation index is a specialization of Eq. (51) obtained by setting $\rho=0$.

The notion of a thin random phase screen is usually predicated on the assumption that only phase fluctuations are impressed on the optical wave as it propagates through the screen. No such assumption was directly imposed here. Rather,

extended turbulence theory was utilized and combined with the assumption that the thickness of the phase screen is small in comparison with the total path length.

Last, the thin phase screen models permit the experimentalist to readily predict statistical results associated with laboratory experiments involving the propagation of a Gaussian-beam wave through a random phase screen and directly relate them to equivalent extended turbulence conditions characteristic of the open atmosphere. To do so, however, requires critical placement of the phase screen with respect to transmitter and receiver.

## Problems

### Section 15.3

1. Use the general result (22) and the large argument asymptotic formula for the confluent hypergeometric function when $\rho > \sqrt{L/k}$ to deduce that

$$\Gamma_2(\mathbf{p},\mathbf{r},L) = \Gamma_2^0(\mathbf{p},\mathbf{r},L)\exp\left[-0.65\hat{\sigma}_R^2\left(\frac{k}{Ld_3}\right)^{5/6}\left|(1-\overline{\Theta}d_3)\mathbf{p} - 2i\Lambda d_3\mathbf{r}\right|^{5/3}\right].$$

2. In the plane wave limit, show that Eq. (23) reduces to the extended turbulence result

$$\Gamma_2(\rho,L) = \exp\left(-1.46C_n^2k^2L\rho^{5/3}\right).$$

3. Use the approximation (57) in Chap. 6 and the asymptotic relation

$${}_1F_1(a;c;-x) \sim 1 - \frac{ax}{c}, \qquad |x| \ll 1,$$

to show that

($a$) the WSF (33) for a thin random phase screen can be approximated by

$$D(\rho,L) \cong 3.87\hat{\sigma}_R^2(\Lambda d_3)^{5/6}\left\{\frac{5k(1-\overline{\Theta}d_3)^2\rho^2}{24\Lambda Ld_3^2}\left[1+0.058\frac{k(1-\overline{\Theta}d_3)^2\rho^2}{\Lambda Ld_3^2}\right]^{-1/6} + \frac{5k\Lambda\rho^2}{24L}\right\}.$$

($b$) For $\rho > \sqrt{L/k}$, show that the expression in part ($a$) further reduces to

$$D(\rho,L) \cong 1.30\hat{\sigma}_R^2d_3^{5/6}\left[\left|\frac{1}{d_3}-\overline{\Theta}\right|^{5/3}\left(\frac{k\rho^2}{L}\right)^{5/6} + 0.62\Lambda^{11/6}\left(\frac{k\rho^2}{L}\right)\right].$$

4. For $\mathbf{r}_1 = \mathbf{r}_2 = \mathbf{r}$, show that Eq. (22) reduces to the result of Eqs. (26)–(28).

### Section 15.4

5. The radial component of the log-amplitude variance associated with a thin phase screen is defined by

$$\sigma_r^2(\mathbf{r},L) = 2\pi^2k^2Ld_2d_3\int_0^\infty \kappa\Phi_n(\kappa)\exp\left(-\frac{\Lambda L\kappa^2d_3^2}{k}\right)[I_0(2\Lambda d_3\kappa r)-1]d\kappa.$$

By use of the Kolmogorov spectrum, derive the approximation

$$\sigma_r^2(\mathbf{r},L) \cong 1.61\hat{\sigma}_R^2(\Lambda d_3)^{5/6}\left(\frac{r^2}{W^2}\right), \quad r < W.$$

6. Given that the longitudinal component of the scintillation index associated with a thin phase screen is defined by

$$\sigma_{I,l}^2(L) = 8\pi^2 k^2 L d_2 d_3 \int_0^\infty \kappa \Phi_n(\kappa) \exp\left(-\frac{\Lambda L \kappa^2 d_3^2}{k}\right) \times \mathrm{Re}\left\{1 - \exp\left[-\frac{iL\kappa^2 d_3}{k}(1 - \overline{\Theta} d_3)\right]\right\} d\kappa,$$

(*a*) show, by expanding the complex exponential function in a Maclaurin series and using the Kolmogorov spectrum, that[1]

$$\sigma_{I,l}^2(L) = 3.87\hat{\sigma}_R^2 (\Lambda d_3)^{5/6}\ \mathrm{Re}\left\{{}_1F_0\left[-\frac{5}{6};—;—\frac{i(1 - \overline{\Theta} d_3)}{\Lambda d_3}\right] - 1\right\}.$$

(*b*) By the use of the identity (GH2) in Appendix I, show that the answer in part (*a*) simplifies to

$$\sigma_{I,l}^2(L) = 3.87\hat{\sigma}_R^2 \left\{\left[(\Lambda d_3)^2 + (1 - \overline{\Theta} d_3)^2\right]^{5/12} \times \cos\left[\frac{5}{6}\tan^{-1}\left(\frac{1 - \overline{\Theta} d_3}{\Lambda d_3}\right)\right] - (\Lambda d_3)^{5/6}\right\}.$$

[1]The absence of a denominator parameter in ${}_1F_0$ is emphasized by a dash.

## References

1. H. G. Booker, "Application of refractive scintillation theory to radio transmission through the ionosphere and the solar wind, and to reflection from a rough ocean," *J. Atmos. and Terres. Phys.* **43**, 1215–1233 (1981).
2. H. G. Booker, J. A. Ferguson, and H. O. Vats, "Comparison between the extended-medium and the phase-screen scintillation theories," *J. Atmos. Terres. Physics* **47**, 381–399 (1985).
3. I. G. Yakushkin, "Intensity fluctuations during small-scale scattering of wave fields," *Radiophys. Quantum Electron.* **28**, 365–389 (1985).
4. L. C. Andrews, R. L. Phillips, and A. R. Weeks, "Propagation of a Gaussian-beam wave through a random phase screen," *Waves Random Media* **7**, 229–244 (1997).
5. A. M. Prokhorov, F. V. Bunkin, K. S. Gochelashvily, and V. I. Shishov, "Laser irradiance in turbulent medium," *Proc. IEEE* **63**, 790–809 (1975).
6. A. Ishimaru, *Wave Propagation and Scattering in Random Media* (IEEE Press, Piscataway, NJ, 1997); [previously published as Vols I & II by Academic, New York (1978)].